Article

pubs.acs.org/Biomac

Effect of pH on Protein Distribution in Electrospun PVA/BSA Composite Nanofibers

Christina Tang, A. Evren Ozcam, Brendon Stout, and Saad A. Khan*

Department of Chemical and Biomolecular Engineering, North Carolina State University, Raleigh, North Carolina 27695, United States

Supporting Information

ABSTRACT: We examine the protein distribution within an electrospun polymer nanofiber using polyvinyl alcohol and bovine serum albumin as a model system. We hypothesize that the location of the protein within the nanofiber can be controlled by carefully selecting the pH and the applied polarity of the electric field as the pH affects the net charge on the proteins. Using fluorescently labeled BSA and surface analysis, we observe that the distribution of BSA is affected by the pH of the electrospinning solution. Therefore, we further probe the relevant forces on the protein in solution during electrospinning. The role of hydrodynamic friction was assessed using glutaraldehyde and HCl as a tool to modify the viscosity of the solution during electrospinning. By varying the pH and the polarity of the applied electric field, we evaluated the effects of electrostatic forces and dielectrophoresis on the protein during fiber formation. We surmise that electrostatic forces and hydrodynamic friction are insignificant relative to dielectrophoretic forces; therefore, it is possible to separate species in a blend using polarizability contrast. A coaxial distribution of protein in the core can be obtained by electrospinning at the isoelectric point of the protein, whereas surface enrichment can be obtained when the protein carries a net charge.

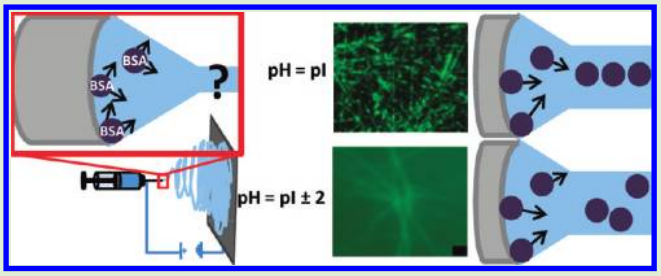

INTRODUCTION

Electrospinning is a simple technique used to generate nanofibrous membranes and nanofiber composites.[1−8] It involves the application of a high voltage (1−30 kV) to induce the formation of a liquid jet of polymer solution or melt. The electrified jet undergoes stretching and whipping resulting in a long and thin fiber. As the liquid jet is continuously extended and the solvent evaporates, there is a significant reduction in the diameter of the jet from several hundred micrometers to as low as tens of nanometers. Eventually, the charged fiber is deposited onto the grounded collector plate as a random, nonwoven mat of nanofibers. The materials produced using this method have exceptional specific surface area and may be of use in a broad range of applications.

In particular, there is increasing interest in protein and protein/polymer composite nanofibers. A number of proteins including bovine serum albumin (BSA), green fluorescent protein, casein, silk, gelatin, lysozyme, cytochrome C, and eggshell membrane protein have been incorporated into electrospun fibers. Generally, proteins must be coelectrospun or coaxially electrospun with an electrospinnable polymer such as polyvinyl alcohol (PVA) or poly(ethylene oxide) (PEO). Additionally, protein nanofibers, namely, BSA and zein, have been electrospun.[9−23]

Such materials are being studied for applications such as tissue engineering, wound healing, drug delivery, and biosensors.[24−28] Depending on the application, the distribution of the protein could greatly affect the performance of the material. For example, in blends used for controlled release, the protein has been placed in the core of the fiber.[29,30] However, in other applications, such as biosensors and catalysts, protein on the surface of the fiber is desired.[31−34] Therefore, considerable efforts have been invested in controlling the distribution of the protein within the fiber, using coaxial electrospinning[35−43] among other approaches. Alternative methods of surface segregation of a homopolymer or functional species within a polymer blend have been achieved by considering surface energy, electric field, or phase separation.[44−48] Recently, Sun et al. have reported using a polarizability contrast to functionalize the surface of electrospun fibers with a peptide segment. The authors found that a PEO block coupled to a model oligopeptide is preferentially driven to the surface during electrospinning of PEO−oligopeptide/PEO and PEO−ologiopeptide/PMMA fibers.[48,49] However, these initial studies are limited to negatively charged peptides. The application of this technique to protein/polymer systems has yet to be established. In this study, we determine how the distribution of protein in a blend fiber is affected during electrospinning by parameters such as solution viscosity, solution pH, and applied polarity of the electric field.

We explore the effect of pH on electrospinning PVA/BSA blends. Because pH affects the net charge on the protein, we

Received: November 30, 2011
Revised: April 7, 2012
Published: April 9, 2012

dx.doi.org/10.1021/bm2017146 | Biomacromolecules 2012, 13, 1269−1278

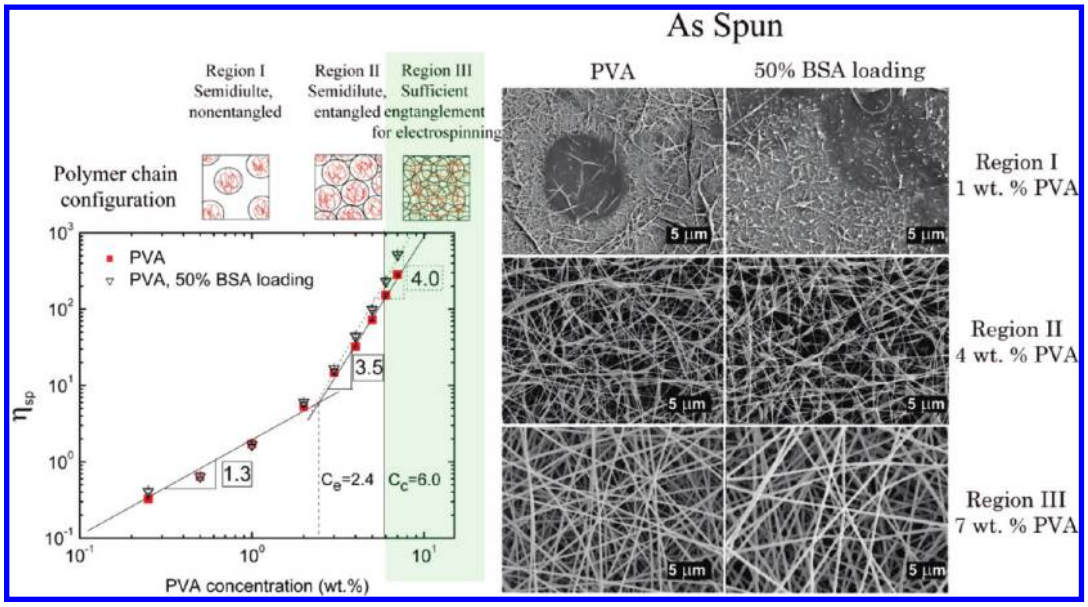

Figure 1. Correlating morphology of electrospun mats with rheological solution properties for PVA/BSA solutions: a log–log plot of η_{sp} vs concentration for solutions of PVA and PVA with 50% BSA loading and SEM images of characteristic fiber morphologies.

suspect that, by carefully choosing the pH of the solution and the applied polarity, the distribution of the protein within the fiber may be modulated. We used glutaraldehyde as a tool to examine the effect of the electrospinning solution viscosity and determine the importance of hydrodynamic friction. By comparing pHs above and below the isoelectric point of BSA and varying the polarity of the applied voltage utilized during electrospinning, we were able to evaluate the relative roles of dielectrophoresis and electrostatic forces. Based on the insight gained, we report the production of a coaxial distribution with protein in the core can be obtained during electrospinning of a blend by carefully selecting the pH of the electrospinning solution.

■ EXPERIMENTAL SECTION

Materials and Methods. *Materials.* Polyvinyl alcohol (PVA; average molecular weight 205000 g/mol, 88% hydrolyzed), hydrochloric acid (HCl; 37% purity), bovine serum albumin (BSA; A-3059, >99%), and fluorescently labeled FITC-BSA (A-9771) were obtained from Sigma Aldrich (St. Louis, MO). Glutaraldehyde (50% aq) was received from Alfa Aesar (Ward Hill, MA). Tris base and sodium hydroxide from Fisher BioReagents (Fair Lawn, New Jersey) and Fisher Scientific (Pittsburgh, PA), respectively, was used. Unconjugated gold colloid (20 nm) was obtained from Ted Pella (Redding, CA). All materials were used as received.

Electrospinning. Aqueous PVA solutions were prepared by stirring mixtures of PVA and deionized water or 50 mM Tris buffer at pH 8.1 at 60 °C until they were homogeneous. BSA was dissolved in Tris buffer, pH 8.1, at room temperature (~25 °C) and stored at 4 °C until further use. PVA and BSA were combined in appropriate proportions at room temperature and stirred briefly. The amount of PVA used is reported as mass of PVA per mass of total solution. The BSA loading is the mass of BSA per mass of PVA. In some cases, the pH of the solutions were adjusted by adding small amounts of HCl and stirring briefly. The pH was measured with a Horiba Twin B-213 pH meter.

To electrospin we used a point-plate configuration, as previously described,[6] where PVA/BSA solution was loaded into a syringe fitted with a stainless steel needle (0.508 mm I.D.) and attached to a power supply (Gamma High Voltage Research, D-ES-30PN/M692). A flow rate of 0.5 mL/hour, collection distance of 15 cm between the tip of the needle and the ground collector plate covered with foil, and applied voltage of 10–22 kV were used. A positive polarity was applied unless otherwise noted.

Viscosity Modulation. Addition of glutaraldehyde and HCl increased the viscosity of the solution over the time for which it was electrospun. In this case, the polymer and protein solutions were combined and stirred briefly, the HCl was added, and the solution was stirred again, and finally, the GA was added in appropriate portions at room temperature and stirred briefly. A portion of the solution was electrospun and another portion tested rheologically immediately after preparation.[49] Electrospun samples were collected for increasing amounts of time and then further characterized.

Rheological Measurements. The zero-shear viscosity of PVA solutions was measured at 25 °C using a TA Instruments AR-G2 Rheometer using a 40 mm diameter, 2° cone and plate geometry. Dynamic oscillatory shear experiments were also performed on selected samples as a function of time at 25 °C using the same rheometer and configuration. A frequency of 10 radians/second and a stress of 1 Pa were used for all experiments because it was within the linear viscoelastic region of the solutions. Measurements of the elastic (G') and viscous (G'') modulus along with loss tangent tan δ (= G''/G') in which δ corresponds to the phase shift, were taken every 30–60 s for up to 24 h.[49] The measurements were stopped with the value of δ falling below 15°, so that the relevant part of the rheology curve was captured, that is, the time required to reach the "gel point".[49]

Sample Characterization. To examine the fiber morphology, samples were sputter coated with an ~10 nm layer of gold and analyzed with a scanning electron microscope (SEM, FEI XL-30) at 5 kV. The average fiber size and standard deviation were determined by measuring the diameter of 100 fibers using ImageJ software. Fibers containing FITC-BSA were imaged with an Olympus BX-61 optical microscope equipped with transmitted- and fluorescence-mode and recorded using an Olympus DP-70 digital CCD camera.

Infrared spectra (4000–400 cm^{-1}) of PVA and PVA/BSA composite samples were measured with a Nicolet 6700 FTIR spectroscope (Thermo Electron Corporation). The surface chemical composition of PVA and PVA/BSA composite samples was determined utilizing XPS with a Kratos Axis Ultra DLD XPS instrument using monochromated Al Kα radiation with charge neutralization. Survey and high-resolution spectra were collected with pass energies of 80 and 20 eV, respectively, using both electrostatic and magnetic lenses. XPS of fibers produced at different pHs and applied polarities were obtained. In the cases where GA and HCl were added to increase the viscosity, samples collected over increasing amounts of time were also evaluated.

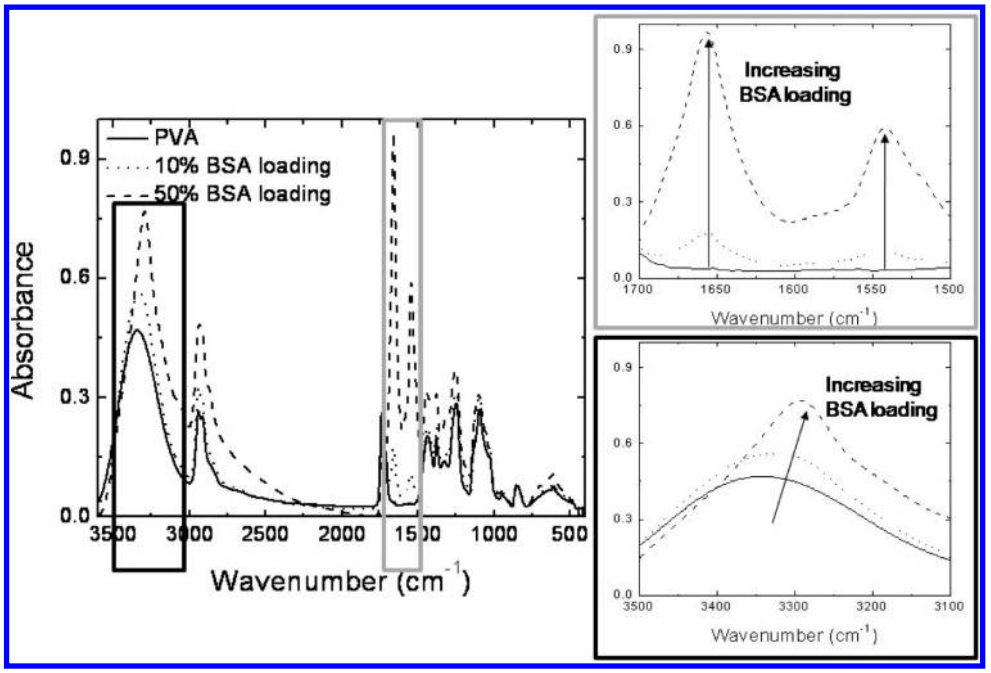

Figure 2. FTIR spectra of PVA and PVA/BSA composite fibers, as spun at room temperature.

Gold Nanoparticle Assay for Protein Visualization on Surfaces. To qualitatively visualize the amount of protein on the surface of fibers, we adsorbed 20 nm colloidal gold particles to chemically cross-linked blend fibers. In this method, 1" squares of electrospun samples were cut and placed in a solution containing 5 vol % glutaraldehyde and 0.12 vol % HCl in acetone based on previously established methods.[21,50,51] PVA/BSA solutions were electrospun for 2 h and cross-linked using GA in acetone with HCl as a catalyst at ambient conditions for 2 h. We then washed the cross-linked fibers thrice in deionized water for 5 min, then soaked in water for 3 h and dried at ambient conditions. Next, the cross-linked samples were submerged in colloidal gold for 48 h at 4 °C. Due to its length, we chose to perform this step at the storage temperature of the protein and the gold colloid (4 °C) to avoid potential denaturing of the protein that could occur over 48 h at room temperature. The samples were removed and washed thrice in water for 5 min, then soaked in water for 3 h and dried at ambient conditions before further analyzing using SEM. From SEM micrographs, the amount of gold in each sample was quantified by particle density. To determine the particle density, the number of particles within a 170 × 290 nm^2 rectangle was manually counted. Measurements were performed 100 times per micrograph using ImageJ software. The statistical significance of the difference in the particle density of different samples was established with a t test (α = 0.05).[52,53]

RESULTS AND DISCUSSION

PVA/BSA Composite Nanofibers. We begin by investigating the effect of the addition of BSA on the electrospinnability of PVA. We correlate solution dynamics with the resulting morphology of the electrospun material, as shown in Figure 1. The solution viscosity, a measure of polymer entanglement, can be used to predict fiber formation of electrospinnable polymers.[54,55] Common fiber morphologies, that is, beaded fibers and uniform fibers, have been correlated with different polymer concentration regions.[55] Figure 1 shows the normalized zero shear viscosity of PVA/BSA solutions as a function of PVA concentration where the BSA loading is held constant at 50% (per weight of PVA). For PVA/BSA blends, below 2 wt % PVA, we find that $\eta_{sp} \sim c^{1.3}$ (where η_{sp} is the specific viscosity and c is the PVA concentration), consistent with the theoretical prediction for semidilute, nonentangled solutions of a neutral polymer in a good solvent.[55−57] Above 3 wt % PVA, $\eta_{sp} \sim c^{3.8}$, characteristic of semidilute entangled solutions.[55−57] The entanglement concentration is 2.5 wt % PVA, as indicated by the change in slope in the η_{sp} versus c plot (Figure 1).[55] As shown by the SEM micrographs in Figure 1, semidilute nonentangled solutions produce discontinuous beaded structures and large droplets; semidilute, entangled solutions produce beaded fibers with increased uniformity when qualitatively compared to nonentangled solutions; concentrations above 6 wt % PVA (C_c, critical concentration) produce uniform fibers. The critical concentration to spin PVA is 6.0 wt %, which is 2.5 times greater than the entanglement molecular weight concentration of 2.4 wt % (Figure 1), which agrees well with previous studies.[54,55]

The presence of BSA (up to 50% loading) does not appear to affect the PVA entanglement required for electrospinning. The addition of the BSA slightly increased the concentration dependence of the specific viscosity in the semidilute entangled regime from 3.5 for PVA to 4.0 for PVA with BSA. The increase in this case may indicate that, at the protein loading used, PVA and protein interact, which has been previously reported and attributed to polar interactions.[21,55] Most importantly, despite PVA/BSA interactions, the presence of the protein does not affect the polymer entanglement necessary for electrospinning; therefore, the electrospinnability of the blends is dictated by PVA entanglement.

We further examined the PVA/BSA blend fibers with FTIR for an indication of the presence of the protein in the fibers (Figure 2). Upon addition of BSA, we note broad peaks between 1500 and 1700 cm^{-1}, and the intensities of the peaks increase with increasing BSA concentration. These peaks likely correspond to the amide I and amide Π bands at 1632 and 1536 cm^{-1}, respectively, of peptide bonds characteristic of BSA. Additionally, we observe a shift in the peak between 3100 and 3500 cm^{-1} toward 3100 cm^{-1}. The degree to which the peak is shifted increases with increasing BSA concentration. These

dx.doi.org/10.1021/bm2017146 | Biomacromolecules 2012, 13, 1269−1278

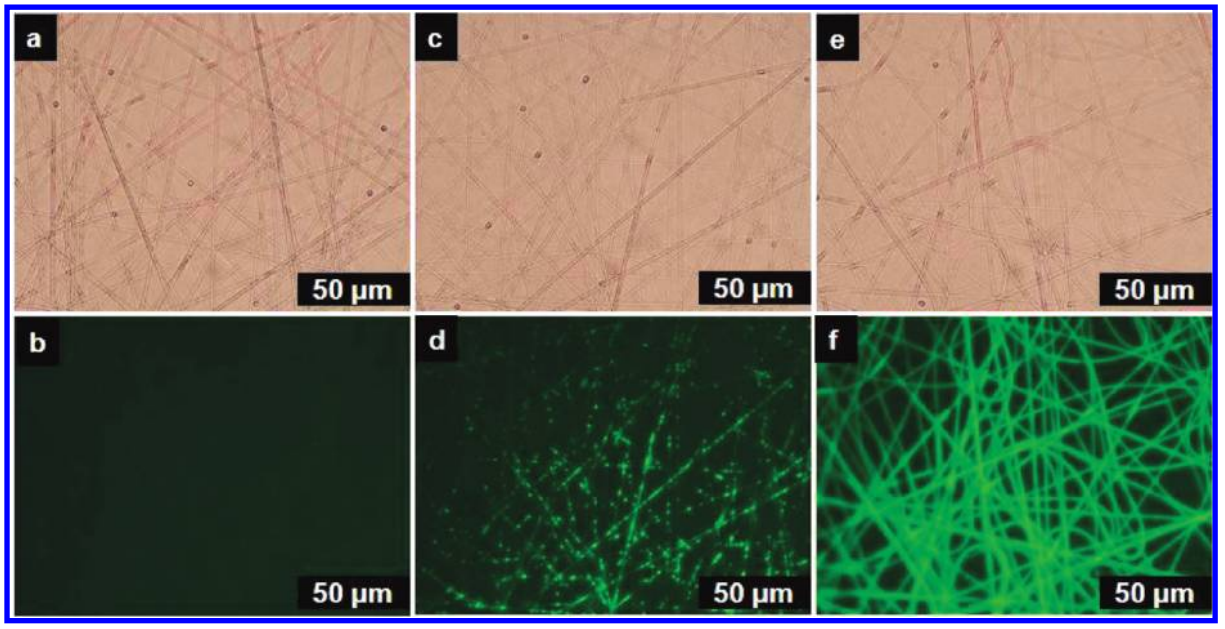

Figure 3. Optical and fluorescence microscopy images of 7 wt % PVA (a) and (b) 0.3% BSA-FITC loading (c) and (d), adjusted to pH 5.0 (pI), and 0.3% BSA-FITC loading (e) and (f), adjusted to pH 8.6.

results agree with previous reports of PVA/protein blend films using soy protein isolate.[58]

Effect of pH. We hypothesized that we could utilize the electrostatic force on a protein carrying a net charge and modulate the distribution of the protein within the fiber by changing the pH of the electrospinning solution as well as the applied polarity of the electric field. At the isoelectric point of BSA (pH 4.7−5.2) there is no net charge on the protein, whereas above the isoelectric point, the protein should carry a net negative charge. If we apply a positive polarity, we would expect the negatively charged protein to be attracted to the surface of the fiber when compared to the case in which the protein carried no net charge. To initially test our hypothesis, we electrospun solutions PVA and fluorescently labeled BSA at a pH above the isoelectric point and at the isoelectric point. In both cases, a positive polarity was applied. We examined the resulting as spun fibers with fluorescence microscopy to determine if we could discern a difference in the distribution of the protein within the fiber in these two cases. We electrospun fibers containing FITC-BSA directly onto glass microscope slides and observed the dry as spun fibers. As a negative control, we examine PVA only fibers under fluorescence at the same conditions to account for background fluorescence. Figure 3 shows protein-loaded nanofibers at various pHs using FITC-labeled BSA. We note that, at a pH (Figure 3d) close to the isoelectric point, we observe some clusters of protein, likely due to protein aggregation. At higher pH (Figure 3f), we do not observe such collections of protein. Interestingly, despite using the same FITC-BSA loading, the fluorescence of fibers produced from a solution of pH 8 (Figure 3f) appears more intense than that of fibers produced from a solution adjusted to the isoelectric point (Figure 3d). Based on the observed differences using fluorescence microscopy, we suspect that the net charge on the protein molecules affects its distribution within the fiber. For example, one contributing factor to the difference in intensity at the different pHs may be that at pH 8 there may be more protein on the surface of the fibers. However, given the size scale of the fibers the information available using optical microscopy techniques is limited. To further investigate the protein distribution within the fiber we examined the protein content on the surface of the fibers.

In the next set of experiments, we attempt to visualize the amount of protein on the surface of the electrospun fibers using SEM as electron microscopy offers higher spatial resolution when compared to optical microscopy. Because fluorescence cannot be used to identify protein on the surface of the fibers, we attempted to use gold nanoparticles to visualize the presence of protein on the surface of the electrospun fibers using SEM. The principle of this method is based on the well-established interactions between proteins and colloidal gold. Binding between colloidal gold and proteins and, more specifically, with BSA, has been previously reported.[58,59] Often proteins are bound to gold surfaces, presumably by electrostatic interactions for applications in biosensors.[60−62] Herein, we use gold to qualitatively assess the surface of PVA/BSA composite fibers. We electrospun PVA/BSA blends and then chemically cross-linked the fibers so that the fibers would be insoluble in colloidal gold. By soaking the cross-linked nanofibers in colloidal gold, the gold nanoparticles bind to the protein present on the surface fibers. We then used SEM to visualize the gold and by proxy the protein on the surface of the fibers.

To assess this approach, we began by simply varying the protein loading. As expected, the amount of gold appears to increase with BSA loading (representative SEM micrographs are shown in Figure 4a−c). The density of particles on the nanofibers increased with increasing BSA loading, as expected. Next, we held the BSA loading constant at 30 wt % and varied the pH (Figure 4d−f). When the pH was adjusted to the pI of the protein, little gold is observed on the surface. In this case, the particle density was not significantly different that the nonspecific binding observed when using PVA only fibers as a negative control. When the pH is adjusted to above the pI of the protein, we do observe gold on the surface. Results from this assay further suggest that a coaxial fiber with protein in the

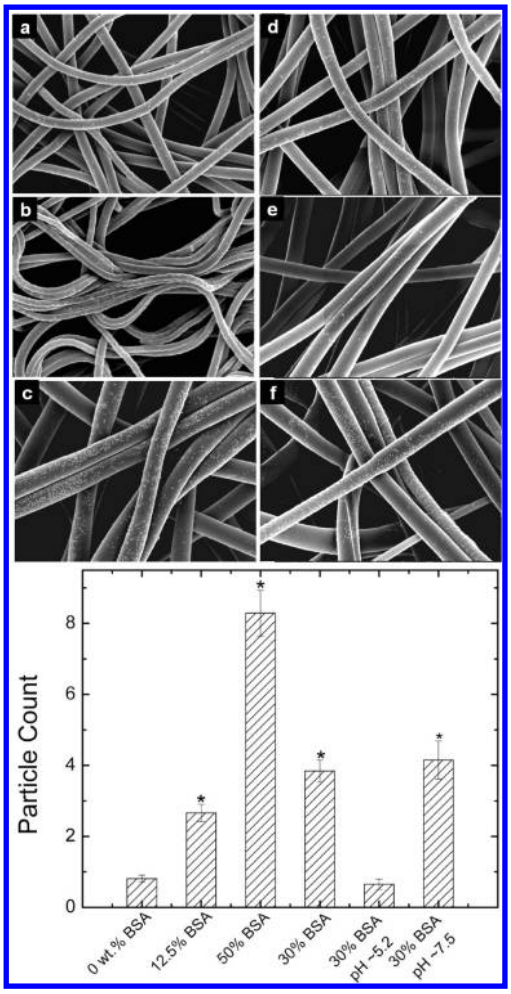

Figure 4. SEM micrographs showing results of a qualitative gold nanoparticle assay of protein concentration on the surface of cross-linked (5 vol % glutaraldehyde, 0.12 vol % HCl in acetone) PVA nanofibers: (a) 7 wt % PVA, (b) 7 wt % PVA with 12% BSA loading, (c) 7 wt % PVA with 50% BSA loading, (d) 7 wt % PVA, 30% BSA loading unadjusted pH, (e) 7 wt % PVA, 30% BSA loading, pH = 5.2 (~pI), and (f) 7 wt % PVA, 30% BSA loading, pH = 7.5. Particle counts for each sample are also shown, * indicates statistically different from the negative control of PVA only (t test, $\alpha = 0.05$).

core is obtained if the pH of the electrospinning solution is adjusted to the isoelectric point of the protein. However, to further confirm this we also use XPS discussed in later sections.

Protein Distribution. Because we do observe that pH can affect the distribution of the protein within the fiber, we next aim to determine if we can control the protein distribution by carefully choosing the net charge on the protein (pH of the electrospinning solution) and the applied polarity. Therefore, we now further probe the relevant forces on the macromolecules in solution during electrospinning with a particular interest in the protein molecule. We first discuss theoretical considerations with simplifications before discussing the experiments results.

During electrospinning, a static, nonuniform electric field is applied to a droplet of a solution. Therefore the forces on a single macromolecule in solution may include (1) electrostatic Coulomb force from an external electric field on a nonzero charged molecule, (2) dielectrophoretic forces due to induced dipole moments in a nonuniform field due to polarizability, and (3) a viscous drag force from hydrodynamic friction. Because we electrospin under ambient conditions, we neglect Brownian motion. We also assume the effect of gravity is negligible since the macromolecules are less than 1 μm in radius.[63,65]

Previous work has developed a model for the DC electric field with a positive applied polarity in a point source to plate electrospinning set up like the one used in our experiments. Results indicate that the highest electric field occurs at the edge of the tip. Further, the average electric field outside the Taylor cone is much higher than the interior which leads to a very high electric field gradient, which may cause dielectrophoresis of the polarizable molecules close to the inner surface of the Taylor cone. Based on the model developed, the Taylor cone area is the most important spot where movement of the polarizable particles occurs. Therefore we consider the forces on the macromolecules in the system within the Taylor cone.[63]

In the case of a protein that carries a net positive or negative charge (i.e., at a pH above or below the isoelectric point of the protein), the distribution of the protein within the Taylor cone during electrospinning may be affected by the applied polarity of the electric field. The applied polarity will affect the charge build up within the Taylor cone, and electrostatic forces on a protein carrying a net charge may cause the charged species to be attracted or repelled from the surface of the Taylor cone based on electrostatic forces, which may influence the distribution of the protein within the final fiber. For example, if the distribution of the protein can be affected by electrostatic forces when a positive polarity is used during electrospinning and the protein carries a net negative charge, we may expect the protein to be attracted the surface of the Taylor cone and thus the fiber. However, if the protein carries a net positive charge we may expect the protein to be repelled from the surface of the Taylor cone resulting in the protein in the core of a core/shell fiber. The force on a single macromolecule in solution will include an electrostatic Coulomb force:

$$F_{Es} = QE = \int_s \sigma_q \mathrm{d}S \cdot E$$

where Q is the total charge on the particle surface, σ_q is the surface charge density, and E is the external electric field strength. The direction of the particle motion will also depend on the charge sign and electric field vector. If the particle is neutral with no net charge, there will be no movement.[63−65]

Further, because a static, nonuniform electric field is applied to a droplet of a solution during electrospinning and we expect the protein to have a very high polarizability, the force on a single macromolecule in polymer solution will also include dielectrophoretic forces due to induced dipole moments in a nonuniform field. The charge density on the inside of the macromolecule relative to the surrounding medium will depend on their relative permittivities. Macromolecules with a higher polarizability than the fluid medium undergo movement toward the electric field region of the strongest intensity. The average dipole moment induced is considered proportional to the vicinity electric field. The polarization is the dipole moment per unit volume (p). The force due to dielectrophoresis is the product of the dipole moment and the electric field gradient.

$$F_{\mathrm{DEP}} = (p \cdot \nabla)E$$

In the case of a DC field, as in the case of electrospinning

$$F_{\mathrm{DEP}} = \frac{1}{4} v 3 \varepsilon_{\mathrm{m}} \left(\frac{\varepsilon_{\mathrm{p}} - \varepsilon_{\mathrm{m}}}{\varepsilon_{\mathrm{p}} + 2\varepsilon_{\mathrm{m}}} \right) \nabla |\mathbf{E}|^2$$

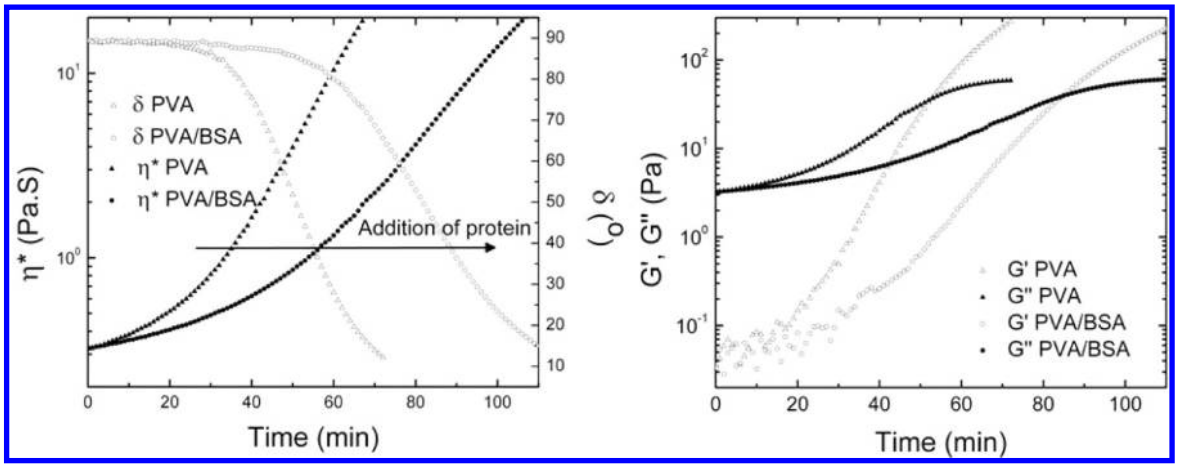

Figure 5. Time-dependent rheology PVA or PVA/BSA solutions after the addition of GA and HCl to either sample of PVA/GA/HCl solutions. Complex viscosity (η^*) and phase angle (δ) evolution with time and viscous (G'') and elastic (G') moduli are shown for a representative sample (7 wt % PVA or 7 wt % with 2.5% BSA loading, 90:1 mol/mol ratio of GA/PVA based on the reported molecular weight of PVA, 10:1 vol/vol ratio GA/HCl).

where v is the volume of the particle, and ε_m and ε_p are the permittivity of the fluid medium and particle, respectively. The force due to dielectrophoresis increases with the electric field and electric field gradient, as well as the polarizability of the particle.[63−65]

Additionally, we consider the drag force on the macromolecule in solution due to hydrodynamic friction. The drag force is proportional to the friction factor and the relative velocity of the macromolecule with respect to the surrounding fluid media. Approximating the macromolecules in solution as spheres, the friction factor is directly proportional to the viscosity of the fluid and radius of the particle. Thus, at high solution viscosities, the drag force will be large and may prevent the ability of the macromolecule to migrate during electrospinning.

$$F_f = f(\mathbf{u} - \mathbf{v})$$

where f is the friction factor, the fluid medium is assumed to move a constant velocity $\mathbf{u}$, and $\mathbf{v}$ is the velocity of the particle. For spherical particles

$$f = 6\pi\eta a$$

where a is the radius of the spherical particle and η is the viscosity of the fluid medium.[63−65]

Another important consideration is if the time scale of electrospinning is sufficient to allow for the macromolecules to migrate within the Taylor cone so that the distribution of the protein within the final fiber is effectively modulated. The velocity of a macromolecule in solution can be estimated by product of the electrophoresis mobility and the electric field strength. For spherical particles, this mobility is proportional to the permittivity and inversely proportional to the viscosity of the fluid medium. The steady state velocity of a neutral macromolecule

$$\mathbf{V}_{DEP} = \frac{F_{DEP}}{f}$$

is thus proportional to the electric field, the electric field gradient, the polarizability of the particle, and inversely proportional to the viscosity. This velocity will have the same vectorial direction as the electric field that is perpendicular to the interface.[63−65]

Hydrodynamic Friction. We first address the role of hydrodynamic friction. Our aim was to ensure that the drag force due to hydrodynamic friction did not prevent the macromolecules from migrating due to the influences of electrostatic forces or dielectrophoresis within the Taylor cone. Further, we wanted to establish that the time scale of electrospinning was sufficient to accommodate sufficient movement due to electrostatic forces and dielectrophoresis to allow for modulation of the protein distribution. Initial indications using fluorescence microscopy and the visualization of gold nanoparticles indicates that drag force due to viscosity would not necessarily prevent a charged protein from migrating to the surface of the fiber. To further investigate the role of hydrodynamic friction, we devised an experiment in which the viscosity of the solution is increasing during electrospinning. By monitoring any changes in surface concentration in parallel with the changes in solution viscosity, we may better understand the role of hydrodynamic friction.

In these experiments, we use the addition of GA and HCl as a tool to modulate the viscosity of the solution during electrospinning. The addition of glutaraldehyde and HCl to a PVA solution immediately prior to electrospinning leads to significant changes in the rheological properties during electrospinning due to cross-linking of PVA.[49] Thus, dynamic rheological properties of the PVA/BSA/H_2O/GA/HCl solutions were monitored as a function of time in parallel with the electrospinning process. Representative profiles of the complex viscosity, viscous modulus, elastic modulus, and delta (a measure of the viscous modulus to the elastic modulus) immediately after the addition of GA and HCl to either PVA or a PVA/BSA blend are shown in Figure 5. We note that, in the time scale shown in Figure 5, the PVA and PVA/BSA samples do not undergo any changes in rheological properties without the addition of both the GA and HCl (data not shown). With the addition of GA and HCl, the systems start out with $G' < G''$ and then become more elastic, where $G' > G''$. When the reaction begins, both G' and G'' increase, but in the same proportion so δ remains constant (~90°). Later, the elastic modulus (G') increases more relative to the increase in the viscous modulus, leading to a decrease in δ. The presence of protein slowed the changes in rheological properties as the onset of the decrease in δ is delayed. The magnitude of the

dx.doi.org/10.1021/bm2017146 | Biomacromolecules 2012, 13, 1269−1278

delay (as measured by the time to reach $\delta = 45°$) increases with BSA loading (Supporting Information, Figure B). The measurements were stopped when the value of δ fell below 15° so that the relevant part of the rheology curve was captured, that is, time required to reach the "gel point" .[49] The delay may be attributed to glutaraldehyde interactions between protein molecules or between protein and polymer, presumably through cross-linking of the ε-amino group of lysyl residues usually on the surface of the protein.[21,66] However, the chemical nature of the reaction between glutaraldehyde and protein is not clearly understood and multiple mechanisms may be involved.[64] Because the GA in the system reacts with the protein, reactions between GA and PVA occur less frequently, thus the change in δ is delayed.

Despite the changes in the rheological properties of the electrospinning solution, we were able to generate uniform PVA/BSA blend fibers (Supporting Information), although we do observe some as spun fibers with a flattened morphology. Flattened fiber morphology suggests an increase in PVA molecular entanglement and effective molecular weight due to GA cross-linking. PVA fibers with similar flattened morphology have been observed and are thought to occur at high molecular weights, because at these high molecular weights relatively wet fibers are deposited on the collector plate due to reduced solvent evaporation and increased viscosity and these wet fibers are flattened on impact.[67]

To evaluate the effect of hydrodynamic friction, which will be proportional to solution viscosity, we examined the surface concentration of nitrogen as a function of time after adding GA and HCl, thereby increasing the solution viscosity, by examining the fiber surfaces deposited at various time intervals (Figure 6). Before the viscosity increases, we expect surface

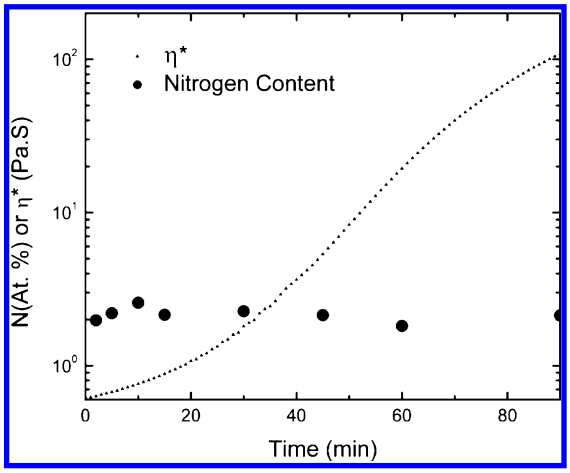

Figure 6. Changes of nitrogen atom surface concentration as measured by XPS and complex viscosity as a function of time after the addition of GA and HCl (7 wt % PVA, 30% BSA loading, pH 2.7).

enrichment to occur due to dielectrophoresis because due to the polarizability of the protein (Figure 6). Additionally, because the pH of the solution is below the isoelectric point and the protein molecule carries a net charge, electrostatic forces may also play a role. Interestingly, despite the viscosity of the solution increasing by over 2 orders of magnitude, there are only small changes in the value of the nitrogen atom surface concentration. From this result, we deduce that the relative magnitude of the drag force due to hydrodynamic friction is small compared to the forces due to dielectrophoresis and electrostatic forces. If the drag force was on the same order of magnitude as the dielectrophoretic force and electrostatic force, as the viscosity increased and the drag force increased, we would have expected to see a drop in protein concentration on the surface as the increased drag force would begin to prevent the protein molecules to migrate to the surface.

From this experiment, we can also gain insight regarding if the time scale of electrospinning is sufficient to allow for segregation within the Taylor cone. We expect the increase in hydrodynamic friction to reduce the velocity at which the proteins are moving within the Taylor cone because the electrophoretic mobility and thus the velocity of the protein is inversely proportional to the viscosity.[63−65] If the time scale were a factor, we would expect that as the viscosity increased and the velocity decreased the surface concentration to drop because the protein molecules would not have sufficient time to seggretate. However, we do not observe the drop despite the increase in viscosity and subsequent decrease in velocity. Therefore, we infer that the time scale of electrospinning is sufficient to facilitate segregation based on either based on electrostatic forces and dielectrophoresis of the macromolecules in the electrospinning solution during electrospinning.[63−65,68] These data imply that drag force on the macromolecules in the Taylor cone due to hydrodynamic friction is small compared to electrostatic and/or dielectrophoretic forces. Thus, we may be able to control the protein distribution within an electrospun fiber by carefully choosing the pH of the electrospinning solution (and resulting net charge on the protein) and the applied electric field.

In this experiment, to modulate the viscosity the pH of the electrospinning solution had to be below the isoelectric point of the BSA and thus BSA was carrying a net charge. In this case, the protein molecules in the Taylor cone were subjected to both electrostatic forces and dielectrophoresis due to the polarizability of the protein molecule. In the next set of experiments, we attempt to determine the relative magnitudes of the electrostatic forces and dielectrophoretic forces.

Electrostatic Forces. We next examine the role of electrostatic forces on the migration of the species within the Taylor cone. We expanded our experiments to include (1) a pH below the isoelectric point resulting in a net positive charge on the protein, (2) a pH at the isoelectric point resulting in no net charge on the protein, and (3) above the isoelectric point resulting in a net negative charge on the protein and also varied the polarity of the voltage applied during electrospinning (positive or negative). At each pH, we examined samples electrospun while applying either a positive polarity or a negative polarity. We expected that if electrostatic forces were dominant, that at a given pH we could force the protein to the surface using one applied polarity and by switching the polarity the electric field we could obtain the opposite distribution with protein within the core of a coaxial fiber. For example, at pHs above the isoelectric point and the protein carries a net negative charge and we applied a positive polarity, as we did in the initial experiments, the negatively charged protein would be driven to the surface of the fiber. However, if we changed the applied polarity to negative, the negatively charged protein would be repelled from the surface of the Taylor cone, resulting in a coaxial fiber with protein in the core.

For each pH and applied polarity, we analyzed the elemental composition of the surface of the fibers using XPS (Figure 7). When electrospinning at the isoelectric point, we do not detect any nitrogen (and thus no protein) on the surface of the fiber.

dx.doi.org/10.1021/bm2017146 | Biomacromolecules 2012, 13, 1269−1278

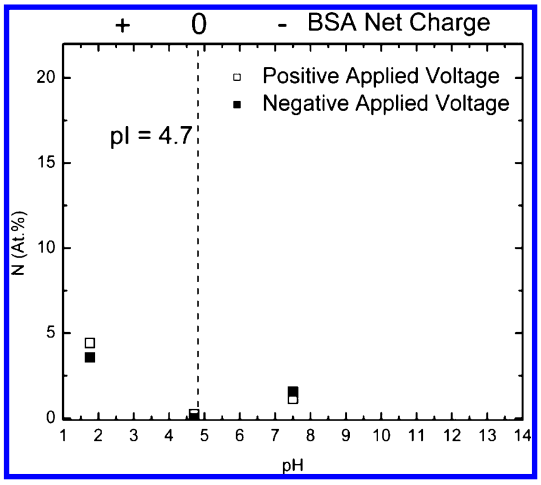

Figure 7. Concentration of nitrogen atoms on the surfaces of fibers produced from 7 wt % PVA, 30% BSA loading as a function of pH, and applied polarity as measured by XPS analysis.

This result suggests a coaxial distribution with protein in the core augmenting the analysis using fluorescence microscopy and the gold nanoparticles to visualize the protein on the surface of the fiber. When we compare the case where the protein carries a net negative charge (above the isoelectric point), we do observe more protein on the surface in the case. This agrees well with the results presented previously using fluorescence microscopy and the gold nanoparticles to visualize the protein on the surface of the fiber (Figures 3 and 4, respectively).

However, when we were using a negatively charged protein and we switched the polarity from positive to negative, we continue to detect protein on the surface. We obtained a similar result when examining a pH below the isoelectric point and the protein carried a net positive charge. If the protein was charged, we observed protein on the surface of the fibers. Most interestingly, despite the charge on the protein, the applied polarity did not greatly affect the surface concentration (Figure 7). This result seems to suggest that electrostatic forces are not the dominant force on the macromolecules in solution during electrospinning.

Dielectrophoretic Forces. Now that we have explored the drag force due to hydrodynamic friction and the electrostatic forces, we will focus on dielectrophoresis. Dielectrophoresis occurs due to polarizability of a macromolecule in the presence of a nonuniform electric field. In dielectrophoresis, macromolecules with a higher polarizability than the fluid medium undergo movement toward the electric field region of the strongest intensity. Because we are studying a blend system that contains the protein and polymer in solution, we must also consider the role of PVA. Therefore, we next consider the effect of pH on PVA, focusing specifically on how pH affects the solution dynamics of PVA.

We have previously established that solution dynamics of PVA in water (pH ~ 5.5) are indicative of a neutral polymer in a good solvent. This is based on the viscosity scaling relationships when plotting specific viscosity vs concentration. Below 2 wt % PVA, $\eta_{sp} \sim c^{1.3}$ (where η_{sp} is the specific viscosity and c is the PVA concentration), and above 3 wt % PVA $\eta_{sp} \sim c^{3.8}$, which is consistent with the theoretical prediction of a neutral polymer in a good solvent. The solution dynamics are shown in Figure 8B for reference and comparison to other pHs.

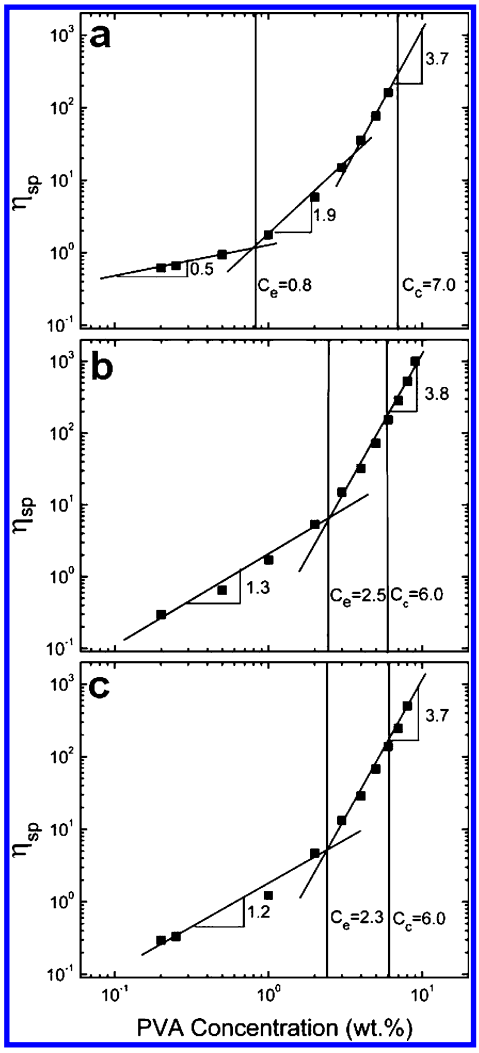

Figure 8. Rheological solution dynamics of PVA: a log−log plot of specific viscosity vs concentration for PVA solutions (a) in Tris buffer, pH 7.5, (b) in DI water, pH 5.5 and (c) pH 2.2, and PVA with 50% BSA loading at (d) pH 8, (e) pH 5, and (f) pH 2.

Further, the entanglement concentration[52,53] was determined to be 2.5 wt % PVA, as indicated by the change in slope in the η_{sp} versus c, and we note the concentration required to electrospin uniform fibers was 2.5 times the entanglement concentration (6.0%), which is expected for a neutral polymer.[54,55] We observe (Figure 8A) similar solution dynamics when the pH is adjusted to 2.2 ($\eta_{sp} \sim c^{1.2}$ below the entanglement concentration, $\eta_{sp} \sim c^{3.7}$ above the entanglement concentration, entanglement concentration 2.4%, uniform fibers produced at 2−2.5 times the entanglement concentration). Based on these results, when the pH of the electrospinning solution is below 5.5, PVA appears to behave as a neutral macromolecule in solution.

Despite the similarity in the behavior in PVA at pHs of 2.2 compared to 5.5, there is a significant difference in the results protein distrubtion. At the isoelectric point (4.7−5.2), both PVA and the protein carry no net charge. In this scenario, we are generating a coaxial fiber with protein in the core by polarizability contrast. This likely occurs because, under these conditions, the PVA molecules are more polarizable that the BSA and are therefore drawn to the surface of the Taylor cone by dielectrophoresis. In contrast, at a pH of 2.2, when the PVA

is neutral but the BSA carries a net positive charge, we do see an indication of protein on the surface of the fiber. Because the positively charged protein is drawn to the surface despite the polarity of the electric field applied, we surmise that the protein at this pH is more polarizable than the PVA and the surface of the fiber is enriched with protein due to dielectrophoresis and polarizability contrast.

We also examined a pH above the isoelectric point. We attempted to increase the pH of the PVA solutions by adding NaOH or even dissolving PVA directly in NaOH, but we found that the pH of these solutions were unstable (when sodium hydroxide was first added the pH would be above 8, but if left for several hours and the pH was remeasured the pH decreased to ~5−6). We were able to make PVA solutions with pH ~7.5 by dissolving PVA in Tris buffer. In Tris buffer, we observe a shift in the solution dynamics (Figure 8C), consistent with the theoretical predictions for polyelectrolytes[69] ($\eta_{sp} \sim c^{0.5}$ below the entanglement concentration, $\eta_{sp} \sim c^{1.9}$ compared to the theoretical prediction of $\eta_{sp} \sim c^{1.5}$ above the entanglement concentration of 0.8 wt %), which indicates the PVA deprotonates at basic pHs. We also note that $\eta_{sp} \sim c^{3.7}$ above 3 wt % PVA, indicating the onset of the concentrated regime. For PVA dissolved in Tris buffer, the critical PVA concentration to form uniform fibers was 7 wt %, slightly higher than 6 wt % for PVA at lower pHs. This result is consistent with previous work electrospinning polyelectrolytes, where concentrations above $8C_e$ were required to generate uniform fibers.[69] Based on these findings, under these conditions, PVA molecules carry a net negative charge presumably due to deprotonation. At this pH (7.5), both the BSA and PVA macromolecules carry a net negative charge. In this case, we observe some protein on the surface due to dielectrophoresis, but not as much as in the case of the acidic pH. This may be attributed to the fact that there is not as much of a difference in polaizability between the BSA in its given form at this pH and the deprotonated form of PVA at this pH. Additionally, this difference may be due to the changes in the tertiary structure of the BSA molecules under the different pH conditions previously reported.[70]

While in reality the forces on the particles in solution are also complicated by particle−particle interactions (probed using solution dynamics of PVA with 50% BSA loading at various pHs, which is provided in Supporting Information, Figure D) and diffusivity, as well as electrostatic diffuse layers surrounding the particles, we can infer the relative roles of dielectrophoresis and Coloumbic forces, as well as drag force on macromolecules in solution during electrospinning, which dictate the distribution of protein within a protein/polymer composite fiber. Based on the results from the viscosity modulation, we deduce that the time scale of electrospinning is sufficient to accommodate segregation by dielectrophoretic/electrostatic forces. Despite significant increases in viscosity and, thus, drag force, the amount of the protein on the surface of fiber was not affected and, thus, the drag force due to hydrodynamic friction is small in comparison to electrostatic and dielectrophoretic forces. Varying the pH of the solution and, thus, the net charge on the protein, as well as the applied polarity, we found the amount of protein on the surface of the fiber at a given pH is not affected by the polarity of the applied electric field. This result indicates that electrostatic forces are not the dominant on a macromolecule in the electrospinning solutions compared to dielectrophoretic forces. At any pH, dielectrophoresis dominates the migration of macromolecules during electrospinning, and based on this understanding, we can capitalize the segregation due to polarizability contrast to vary the distribution of the protein within the electrospun fiber for a given application. To obtain a coaxial distribution, with protein in the core, the pH of the electrospinning solution should be adjusted to the isoelectric point of the protein. When electrospinning at the isoelectric point, the pH at which the protein molecule has no net charge, the PVA molecules appear more polarizable than the protein and, thus, experience more electrophoretic forces and are drawn to the surface of the fiber. This provides a possible single-step method to producing coaxial fibers with a protein core and polymer shell.

CONCLUSIONS

We find that the addition of a model globular protein, BSA, does not affect the molecular entanglement required to electrospin PVA and we were able to incorporate up to 50% BSA loading (per weight of PVA). Further, pH of the electrospinning solution affected the surface concentration of the protein, as indicated by XPS and a quantitative colloidal gold assay, to visualize the protein on the surface. To further understand why protein distribution was affected by pH, we explored the effects of dielectrophoresis, electrostatic forces, and hydrodynamic friction during electrospinning. We deduce that electrostatic forces and hydrodynamic friction are small relative to dielectrophoretic forces. Based on this understanding, we can utilize polarization contrast as a strategy to modulate the protein distribution within the fiber: a coaxial distribution with protein in the core can be obtained by electrospinning at the isoelectric point of the protein when the polymer molecules are drawn to the surface due to their relative polarizability. Alternatively, surface enrichment occurs when the protein carries a net charge and is more polarizable than the polymer.

ASSOCIATED CONTENT

Supporting Information

Fiber size as a function of protein loading, as well as cross-linking reaction kinetics, as measured by changes in rheological properties as a function of protein loading, representative SEM images of PVA electrospun at different pHs, and solution dynamics of PVA/BSA system at different pH values are available. This material is available free of charge via the Internet at http://pubs.acs.org.

AUTHOR INFORMATION

Corresponding Author

*E-mail: khan@eos.ncsu.edu. Tel.: 919-515-4519.

Notes

The authors declare no competing financial interest.

ACKNOWLEDGMENTS

This work was supported by the U.S. Department of Education Graduate Assistance in Areas of National Need (GAANN) Fellowship Program at North Carolina State University. The authors thank Dr. Orlin Velev and J. Kleinert for their assistance with fluorescence microscopy.

REFERENCES

(1) Burger, C.; Hsiao, B. S.; Chu, B. *Annu. Rev. Mater. Res.* **2006**, *36*, 333−368.
(2) Li, D.; Xia, Y. *Adv. Mater.* **2004**, *16*, 1151−1170.
(3) Reneker, D. H.; Chun, I. *Nanotechnology* **1996**, *7*, 216−223.

(4) Huang, Z.; Zhang, Y. Z.; Kotaki, M.; Ramakrishna, S. *Compos. Sci. Technol.* **2003**, *63*, 2223−2253.
(5) Fridrikh, S. V.; Yu, J. H.; Brenner, M. P.; Rutledge, G. C. *Phys. Rev. Lett.* **2003**, *90*, 144502−1−4.
(6) Saquing, C.; Manasco, J. L.; Khan, S.A.. *Small* **2009**, *5*, 944−951.
(7) Gupta, A.; Saquing, C. D.; Afshari, M.; Tonelli, A. E.; Khan, S. A.; Kotek, R. *Macromolecules* **2009**, *42*, 709−715.
(8) Talwar, S.; Hinestroza, J.; Pourdehimi, B.; Khan, S. A. *Macromolecules* **2008**, *41*, 4275−4283.
(9) Xie, J.; Hsieh, Y. L. *J. Mater. Sci.* **2003**, *38*, 2125−2133.
(10) Zhang, C.; Yuan, X.; Wu, L.; Han, Y.; Sheng, J. *Eur. Polym. J.* **2005**, *41*, 423−432.
(11) Greiner, A.; Wendorff, J. H.; Yarin, A. L.; Zussman, E. *Appl. Microbiol. Biotechnol.* **2006**, *71*, 387−393.
(12) Yi, F.; Guo, Z.; Hu, P.; Fang, Z.; Yu, J.; Li, Q. *Macromol. Rapid Commun.* **2004**, *25*, 1038−1043.
(13) Yao, C.; Li, X.; Song, T. *J. Appl. Polym. Sci.* **2007**, *103*, 380−385.
(14) Torres-Giner, S.; Gimenez, E.; Lagaron, J. M. *Food Hydrocolloid.* **2008**, *22*, 601−614.
(15) Min, B.; Lee, G.; Kim, S. H.; Nam, Y. S.; Lee, T. S.; Park, W. H. *Biomaterials* **2004**, *25*, 1289−1297.
(16) Huang, Z.; Zhang, Y. Z.; Ramakrishna, S.; Lim, C. T. *Polymer* **2004**, *45*, 5361−5368.
(17) Dror, Y.; Ziv, T.; Makarov, V.; Wolf, H.; Admon, A; Zussman, E. *Biomacromolecules* **2008**, *9*, 2749−2754.
(18) Sawicka, K.; Gouma, P.; Simon, S. *Sens. Actuators, B* **2005**, *108*, 585−588.
(19) Ren, G.; Xu, X.; Liu, Q.; Cheng, J.; Yuan, X.; Wu, L.; Wan, Y. *React. Funct. Polym.* **2006**, *66*, 1559−1564.
(20) Herricks, T. E.; Kim, S.; Kim, J.; Li, D.; Kwak, J. H.; Grate, J. W.; Kim, S. H.; Xia, Y. *J. Mater. Chem.* **2005**, *15*, 3241−3245.
(21) Wang, Y.; Hsieh, Y. L. *J. Membr. Sci.* **2008**, *309*, 73−81.
(22) Wu, L.; Yuan, X.; Sheng, J. *J. Membr. Sci.* **2005**, *250*, 167−173.
(23) Wang, Z.; Wan, L.; Liu, Z.; Huang, X.; Xu, Z. *J. Mol. Catal. B: Enzym.* **2009**, *56*, 189−195.
(24) Ramakrishna, S.; Lala, N. L.; Garudadhwaj, H.; Ramaseshan, R.; Ganesh, V. K. Polymer Nanofibers for Biosensor Applications; Molecular Building Blocks for Nanotechnology, Molecular Building Blocks for Nanotechnology From Diamondoids to Nanoscale Materials and Applications. Book Series. *Topics in Applied Physics*; Mansoori, G. A., George, T. F., Assoufid, L., Zhang, G., Eds.; Springer: Berlin/Heidelberg, 2007; Vol. *109*, pp 377−392.
(25) Agarwal, S.; Wendorff, J. H.; Greiner, A. *Polymer* **2008**, *49*, 5603−5621.
(26) Agarwal, S.; Wendorff, J. H.; Greiner, A. *Adv. Mater.* **2009**, *21*, 3343−3351.
(27) Cui, W.; Zhour, Y.; Chang. *J. Sci. Technol. Adv. Mater.* **2010**, *11*, 014108.
(28) John, M. J.; Thomas, S. *Carbohydr. Polym.* **2008**, *71*, 343−364.
(29) Choi, J. S.; Choi, S. H.; Yoo, H. S. *J. Mater. Chem.* **2011**, *21*, 5358−5267.
(30) Su, Y.; Su, Q.; Liu, W.; Jin, G.; Mo, X.; Ramakrishna, S. *J. Biomater. Sci., Polym. Ed.* **2011**, *10*, 1−11.
(31) Scampicchio, M.; Arecchi, A.; Bianco, A.; Bulbarello, A.; Bertarelli, C.; Mannino, S. *Electroanalysis* **2010**, *22*, 1056−1060.
(32) Arecchi, A.; Scampicchio, M.; Drusch, S.; Mannino, S. *Anal. Chim. Acta* **2010**, *659*, 133−136.
(33) Li, S.; Wu, W. *Biochem. Eng. J.* **2009**, *45*, 48−53.
(34) Lee, S; Jin, L. H.; Kim, J. H.; Han, S. O.; Na, H. B.; Hyeon, T.; Koo, Y.; Kim, J.; Lee, J. *Bioprocess Biosyst. Eng.* **2010**, *33*, 141−147.
(35) Maretschek, S.; Greiner, A.; Kissel, T. *J. Controlled Release* **2008**, *127*, 180−187.
(36) Chew, S. Y.; Wen, J.; Yim, E. K. F.; Leong, K. W. *Biomacromolecules* **2005**, *6*, 2017−2024.
(37) Kim, T. G.; Lee, D. G.; Park, T. G. *Int. J. Pharm.* **2007**, *338*, 276−283.
(38) Jiang, H.; Hu, Y.; Li, Y.; Zhao, P.; Zhu, K.; Chem, W. *J. Controlled Release* **2005**, *108*, 237−243.
(39) Liao, I. C.; Chew, S. Y.; Leong, K. W. *Nanomedicine (London, U.K.)* **2006**, *1*, 465−471.
(40) Jiang, H.; Hi, Y.; Zhao, P.; Li, Y.; Zhu, K. *J. Biomed. Mater. Res. B* **2006**, *79B*, 50−57.
(41) Schiffman, J. D.; Schauer, C. L. *Biomacromolecules* **2007**, *8*, 2665−2667.
(42) Yang, E.; Qin, X.; Wang, S. *Mater. Lett.* **2008**, *62*, 3555−3557.
(43) Dror, Y.; Kuhn, J.; Avrahami, R.; Zussman, E. *Macromolecules* **2008**, *41*, 4187−4192.
(44) Sanders, E. H.; Klowfkorn, R.; Bowlin, G. L.; Simpson, D. G.; Wnek, G. E. *Macromolecules* **2003**, *26*, 3803−3805.
(45) Bazilevsky, A. V.; Yarin, A. L.; Megaridis, C.M.. *Langmuir* **2007**, *23*, 2311−2314.
(46) Qi, H.; Hu, P.; Xu., J.; Wang, A. *Biomacromolecules* **2006**, *7*, 2327−2330.
(47) Sun, X.; et al. *Adv. Mater.* **2007**, *19*, 87−91.
(48) Sun, X.; Shankar, R.; Borner, H. G.; Ghosh, T. K.; Spontak, R. J. *Macromol. Rapid Commun.* **2008**, *29*, 1455−1460.
(49) Tang, C.; Saquing, C. D.; Harding, J. R.; Khan, S. A. *Macromolecules* **2010**, *43*, 630−637.
(50) Wang, X.; Chen, X.; Yoon, K; Fang, D.; Hsiao, B. S.; Chu, B. *Environ. Sci. Technol.* **2005**, *39*, 7684−7691.
(51) Kim, K.; Lee, S.; Han, N. *Korean J. Chem. Eng.* **1994**, *11*, 41−47.
(52) Bhat, R. R.; Genzer, J. *Nanotechnology* **2007**, *18* (025301), 6pp.
(53) Talwar, S.; Hinestroza, J.; Pourdeyhimi, B.; Khan, S. A. *Macromolecules* **2008**, *41*, 4275−4283.
(54) Shenoy, S. L.; Bates, W. D.; Frisch, H. L.; Wnek, G.E.. *Polymer* **2005**, *46*, 3372−3384.
(55) McKee, M. G.; Wilkes, G. L.; Colby, R. H.; Long, T.E.. *Macromolecules* **2004**, *37*, 1760−1767.
(56) Klossner, R. R.; Queen, H. A.; Coughlin, A. J.; Krause, W. E. *Biomacromolecules* **2008**, *9*, 2947−2953.
(57) Dobrynin, A. V.; Colby, R. H.; Rubinstein, M. *Macromolecules* **1995**, *28*, 1856−1871.
(58) Su, J.; Huang, Z.; Yang, C.; Yuan, X. *J. Appl. Polym. Sci.* **2008**, *110*, 3706−3716.
(59) Horovitz, O.; Tomoaia, G.; Mocanu, A.; Yupsanis, T.; Tomoais-Cotisel, M. *Gold Bull.* **2007**, *40*, 213−218.
(60) Brewer, S. H.; Glomm, W. R.; Johnson, M. C.; Knag, M. K.; Franzen, S. *Langmuir* **2005**, *21*, 9303−0307.
(61) Liu, S.; Leech, D.; Ju, H. *Anal. Lett.* **2003**, *36*, 1−19.
(62) Haes, A. J.; Stuart, D. A.; Nie, S.; Van Duyne, R. P. *J. Fluoresc.* **2004**, *14*, 355−367.
(63) Sun, X. Concurrent and Sequential Surface Modification of Electrospun Polymer Micro/Nano-Fibers. *Ph.D. Dissertation*, North Carolina State University, Raleigh, NC, April 2009.
(64) Grant, E. H.; Sheppard, R. J.; South, G. P. *Dielectric Behavior of Molecules in Soluton*; Carendon Press: Oxford, 1978.
(65) Dukin, S. S.; Shilov, V. N. *Dielectric Phenomena and the Double Layer in Disperse Systems and Polyelectrolytes*; Wiley: New York, 1974.
(66) Migneault, I.; Dartiguenave, C.; Bertrand, M.; Waldron, K. C. *BioTechniques* **2004**, *37*, 790−802.
(67) Koski, A.; Yim, K.; Shivkumar, S. *Mater. Lett.* **2004**, *58*, 493−497.
(68) Velev, O. D.; Gangwal, S.; Petsev, D. N. *Annu. Rep. Prog. Chem., Sect. C* **2009**, *105*, 213−246.
(69) McKee, M. G.; Hunley, M. T.; Layman, J. M.; Long, T. E. *Macromolecules* **2006**, *39*, 575−583.
(70) Bohme, U.; Scheler, U. *Chem. Phys. Lett.* **2007**, *435*, 342−345.